

## Article

# Multi-Variable SWAT Model Calibration Using Satellite-Based Evapotranspiration Data and Streamflow

Evgenia Koltsida and Andreas Kallioras \* 

Laboratory of Engineering Geology and Hydrogeology, School of Mining and Metallurgical Engineering, National Technical University of Athens, Heroon Polytechniou Str. 9, 15780 Athens, Greece; [ekoltsida@metal.ntua.gr](mailto:ekoltsida@metal.ntua.gr)

\* Correspondence: [kallioras@metal.ntua.gr](mailto:kallioras@metal.ntua.gr); Tel.: +30-210-772-2098

**Abstract:** In this study, monthly streamflow and satellite-based actual evapotranspiration data (AET) were used to evaluate the Soil and Water Assessment Tool (SWAT) model for the calibration of an experimental sub-basin with mixed land-use characteristics in Athens, Greece. Three calibration scenarios were performed using streamflow (i.e., single variable), AET (i.e., single variable), and streamflow–AET data together (i.e., multi-variable) to provide insights into how different calibration scenarios affect the hydrological processes of a catchment with complex land use characteristics. The actual evapotranspiration data were obtained from the Moderate Resolution Imaging Spectroradiometer (MODIS). The calibration was achieved with the use of the SUFI-2 algorithm in the SWAT-CUP program. The results suggested that the single variable calibrations showed moderately better performance than the multi-variable calibration. However, the multi-variable calibration scenario displayed acceptable outcomes for both streamflow and actual evapotranspiration and indicated reasonably good streamflow estimations (NSE = 0.70;  $R^2 = 0.86$ ; PBIAS = 6.1%). The model under-predicted AET in all calibration scenarios during the dry season compared to MODIS satellite-based AET. Overall, this study demonstrated that satellite-based AET data, together with streamflow data, can enhance model performance and be a good choice for watersheds lacking sufficient spatial data and observations.

**Keywords:** SWAT; streamflow; MODIS; evapotranspiration; hydrological modeling; multi-variable calibration



**Citation:** Koltsida, E.; Kallioras, A. Multi-Variable SWAT Model Calibration Using Satellite-Based Evapotranspiration Data and Streamflow. *Hydrology* **2022**, *9*, 112. <https://doi.org/10.3390/hydrology9070112>

Academic Editors: Tommaso Caloiero, Carmelina Costanzo and Roberta Padulano

Received: 26 April 2022

Accepted: 17 June 2022

Published: 21 June 2022

**Publisher's Note:** MDPI stays neutral with regard to jurisdictional claims in published maps and institutional affiliations.



**Copyright:** © 2022 by the authors. Licensee MDPI, Basel, Switzerland. This article is an open access article distributed under the terms and conditions of the Creative Commons Attribution (CC BY) license (<https://creativecommons.org/licenses/by/4.0/>).

## 1. Introduction

Hydrological models have been extensively utilized to estimate the consequences of climate variability, land management practices, and policy directions at various temporal and spatial scales [1]. Model development requires a good comprehension of the watershed characteristics to achieve accurate model simulation [2,3]. Nonetheless, most basins are ungauged or inadequately gauged [4]. The absence of adequate observations affects the calibration process and further model improvement [5].

Hydrological model calibration is typically achieved with flow data at the outlet of the basin by choosing the most suitable values for input parameters and comparing simulated outcomes with observed data [6]. However, calibration focused on one variable only may aggregate all watershed processes together and intensify the occurrence of the equifinality problem (i.e., multiple parameter sets can reproduce a similar output) [7–9]. Using multiple variables (e.g., streamflow, evapotranspiration, soil moisture) in the calibration process attempts to overcome equifinality across multiple parameter sets [10–12].

In addition, unknown procedures to the modeler, such as unidentified discharges, agricultural activities, and dumping of construction materials, interfere with the natural behavior of the system and increase the uncertainty in streamflow calibration [13,14]. Therefore, incorporating remote sensing data in model calibration can increase model accuracy, capture the spatial and temporal heterogeneity of hydrological processes, and be a promising

alternative for catchments lacking sufficient observations [13,15,16]. Satellite-based actual evapotranspiration (AET) data can be used to constrain hydrological parameters associated with the water balance [17,18]. For instance, a study in southern India [13] used MODIS satellite-based AET data to calibrate the SWAT model and suggested that satellite-based AET data with a monthly temporal resolution can be used to reduce equifinality obtained from traditional streamflow calibration. In addition, a study in Myanmar [16] calibrated the SWAT model using (Global Land Evaporation Amsterdam Model (GLEAM) satellite-based AET data and measured streamflow. This study suggested that constraining the model with actual evapotranspiration and streamflow data (i.e., multi-variable calibration) can produce good results for both variables. Finally, a study in a catchment in Michigan [18] calibrated the SWAT model using observed streamflow data and remotely sensed based AET data from the Simplified Surface Energy Balance (SSEBop) model and the Atmosphere-Land Exchange Inverse (ALEXI) model. The results of this study suggested that incorporating satellite-based AET data in the hydrological model calibration can maintain a satisfactory performance for streamflow while improving evapotranspiration estimations.

The complexity of spatially distributed model applications in mixed land-use watersheds (i.e., blended combinations of land use) has been explored in past studies [19–23]. Nevertheless, the use of remote sensing data for hydrological model calibration in mixed land-use watersheds has not yet been thoroughly analysed. Urban and peri-urban environments are characterized by high variability in land use, soil types, management practices, and diverse hydrological processes, which increase issues of model uncertainties and make the calibration process challenging [20,24]. The SWAT model is a physically-based model that incorporates the spatial distribution of land use, topography, and soil and allows different hydrological processes in a watershed to interconnect [6]. This makes the model able to estimate how the hydrological components are affected by land management methods in catchments with complex land uses and heterogeneity in soil formations. This study used streamflow and satellite-based actual evapotranspiration (AET) data to calibrate the SWAT model of an urban/peri-urban catchment characterized by a typical Mediterranean climate. Three calibration scenarios were developed using (i) streamflow data, (ii) AET data, and (iii) both streamflow and AET data. This study aims to (i) investigate which parameters are more sensitive in the single variable and multi-variable scenarios; (ii) assess the model performance of the different scenarios; (iii) examine the outcomes of major hydrological components between the single-variable and multi-variable scenarios, and (iv) evaluate the suitability of remote sensing data for streamflow simulation. This study is the first attempt to simulate the hydrological components of an experimental sub-basin with complex land use characteristics and will provide insights into how different calibration scenarios affect the hydrological processes for sustainable water resource management. The major innovation of the proposed methodology is that it has been developed for a typical Mediterranean peri-urban area and can be easily applied to catchments with similar hydrological and geomorphological characteristics.

## 2. Materials and Methods

### 2.1. Description of the Study Area

The study site is a sub-basin (140 km<sup>2</sup>) of the Kifissos River basin (380 km<sup>2</sup>), Athens, Greece (Figure 1). The Kifissos River's route is almost 22 km, of which at least 14 km are within an urban area [25]. The elevation varies from 1399 m in the northern part to 94 m in the southern part. The study area has a mild Mediterranean climate [26]. The mean annual temperature is 16.4 °C, and the mean annual rainfall is 643 mm [27]. The mean annual actual evapotranspiration is 483 mm. The annual evapotranspiration ranges from 551 mm (upstream) to 395 mm (downstream) (Figure 2a).

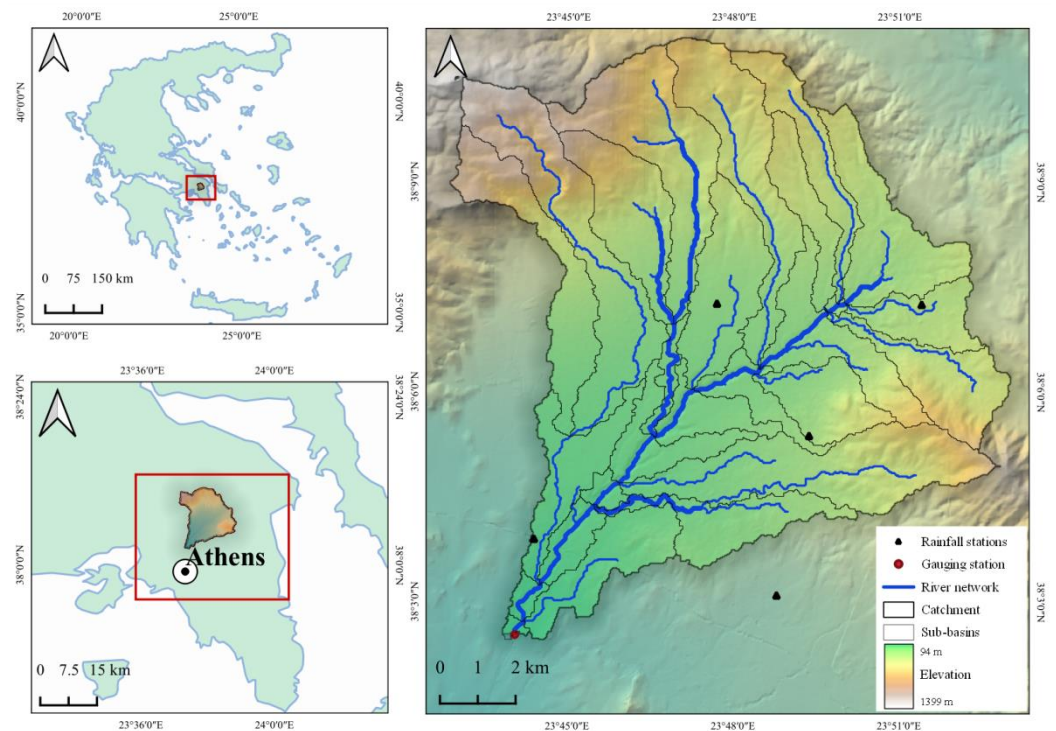


**Figure 1.** Location of Kifissos River sub-basin and monitoring stations (right), Athens metropolitan area (lower left), and zoom out display of Greece (upper left).

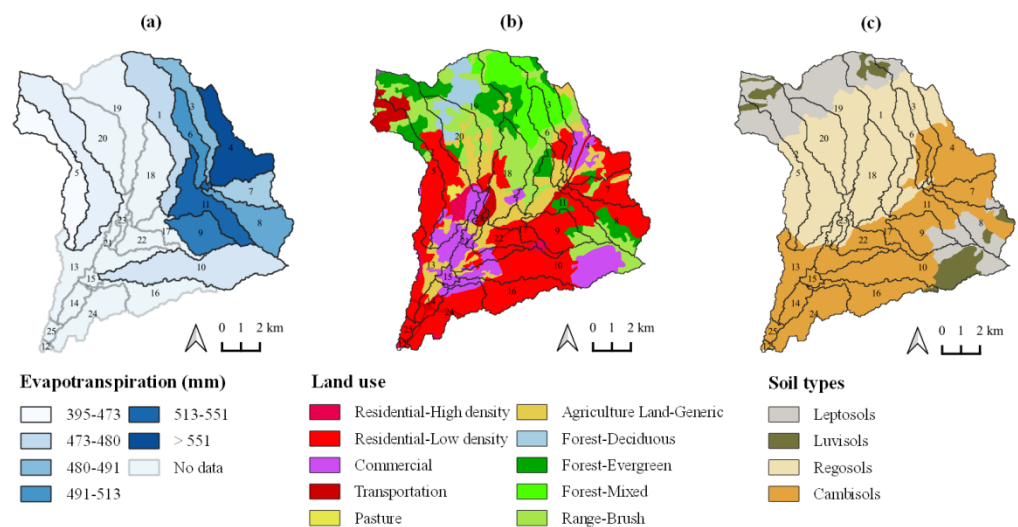


**Figure 2.** Kifissos River sub-basin (a) MODIS average annual evapotranspiration, (b) land use, and (c) soil types. The study area includes 25 sub-basins of which the sub-basin numbers (1–11) indicate the sub-basins used for actual evapotranspiration calibration.

The sub-basin is an urban/peri-urban area. The dominant land cover types are residential areas (34.1%), shrubland (15.9%), and agriculture (12.4%) (Figure 2b) [28]. Table A1 displays the land use categories of the study area at catchment level and Table A2 displays the land use categories of the study area at sub-basin level. The major soils are Cambisols, Regosols, Leptosols, and Luvisols [29]. These formations are generally high in clay and sand contents with good soil permeability (Figure 2c).

## 2.2. Data Sources

The input data include a digital elevation model (DEM) at 30 m resolution from the website of the US Geological Survey [30], a land use map from the 100 m 2018 Corine

Land Cover map [28], a soil map from the Food and Agriculture Organization Digital Soil Map of the World (30 arcseconds resolution) [31], and meteorological data from the National Observatory of Athens [27]. Daily rainfall data were obtained from 2015 to 2019. The daily measured streamflow data at the basin outlet (Monastiri gauging station) were available from 2018 to 2019 and were retrieved from Open Hydrosystem Information Network [32]. The actual evapotranspiration (AET) data were collected from the Moderate Resolution Imaging Spectroradiometer Global Evaporation [33] with a pixel resolution of  $500 \times 500$  m [34].

### 2.3. The SWAT Hydrological Model

The SWAT (Soil and Water Assessment Tool) program is an open-source, physically based, continuous-time river basin model developed to estimate the influence of management practices on discharge, sediments, and agriculture in large complex basins [6,35]. The model runs on a daily time step, and its main variables are hydrology, weather, soil, land use, sediments, nutrients, bacteria, and pathogens.

In SWAT, the basin is divided into sub-basins, then into hydrologic response units (HRUs) with unique land use, soil, and slope characteristics [36]. The water balance is computed separately for each hydrologic response unit [37]. The water balance equation is estimated using the following (Equation (1)):

$$SW_t = SW_o + \sum_{i=1}^t (R_{day} - Q_{surf} - E_a - W_{seep} - Q_{gw}), \quad (1)$$

where  $SW_t$  is the soil water content (mm),  $SW_o$  is the soil water content on day  $i$  in the previous period (mm),  $t$  is the time step (days),  $R_{day}$  indicates the amount of precipitation on day  $i$  (mm),  $Q_{surf}$  represents the surface streamflow on day  $i$  (mm),  $E_a$  indicates the AET on day  $i$  (mm),  $W_{seep}$  is the percolation and bypass flow on day  $i$  (mm), and  $Q_{gw}$  represents the return flow on day  $i$  (mm).

### 2.4. Model Setup

The QGIS interface of the SWAT model was utilized for model configuration [38]. The watershed was delineated into 25 sub-basins and 386 hydrological response units (HRUs). A 10% threshold was used for land use, soil, and slope to limit the influence of minor soil and land use types for each sub-basin. The Corine Land Cover land use classes [28] were converted to the SWAT land use classes [6]. The model was simulated from 2015 to 2019 and run on a daily time step. Two years (1 January 2015–31 December 2016) were set as a warm-up period. The potential evapotranspiration was calculated using the Penman–Monteith method, the surface runoff was estimated using the curve number method [39], and the channel routing was computed using the variable storage coefficient method [40].

### 2.5. Model Calibration and Sensitivity Analysis

The model was calibrated using the Sequential Uncertainty Fitting Algorithm (SUFI-2) in the SWAT-Calibration and Uncertainty Program (SWAT-CUP) [41]. In SUFI-2, the calibrating parameters are set according to literature and sensitivity analysis, and then the parameters sets are generated using Latin hypercube sampling (LHS) [14]. The significance of each parameter is defined with a  $t$ -test. Parameters with large  $t$ -stat and small  $p$ -value ( $p$ -value  $< 0.03$ ) are identified as sensitive parameters [42].

Three calibration scenarios were conducted using monthly time series of streamflow from one station at the outlet of the study site and the MODIS satellite-based actual evapotranspiration (AET) from eleven sub-basins based on data availability [33]. The daily streamflow was converted to monthly for comparison reasons. The monthly average values were calculated by a resample function, and the missing values were estimated by an interpolation function using the linear method (Python pandas library). The actual evapotranspiration data from MODIS were in a geotiff format (raster). In addition, to compare the MODIS satellite-based AET (pixel values) to the SWAT simulated AET, an

area-weighted averaging approach in QGIS (zonal statistics) was performed to create the aggregated monthly values for each sub-basin [23,43].

The scenarios include: (i) streamflow calibration (i.e., single variable), (ii) AET calibration (i.e., single variable), and (iii) both streamflow and AET calibration (i.e., multi-variable). Based on data availability, streamflow was calibrated from 2018 to 2019, and evapotranspiration was calibrated from 2017 to 2019. All the available data were used for model calibration to represent the wet and dry conditions properly (2017: 487 mm, 2018: 675 mm, 2019: 765 mm). The calibration process used 20 parameters linked to streamflow and evapotranspiration (Table 1), and their sensitivities were estimated. The original value ranges of the parameters and their sensitivities for each calibration scenario are displayed in Table 2. In the single variable calibrations, the two variables (i.e., streamflow and actual evapotranspiration) were calibrated separately, and the performance of the second variable was evaluated. In the multi-variable calibration the two variables were calibrated together using a multi-variable objective function and assigning equal weights to each variable [16,44]. The Nash–Sutcliffe model efficiency (NS) was used as an objective function, and 900 simulations per iteration were performed and up to three iterations.

**Table 1.** Calibrated parameters. The method “r” (relative) indicates multiplying the current parameter value by a given value, the method “v” (replace) indicates replacing the current parameter value, and the method “a” (absolute) indicates adding a given value to the current parameter [14].

Category	Parameter	Description
Surface runoff	r_CN2.mgt	Curve number
	v_SURLAG.bsn	Surface runoff lag coefficient
Groundwater/Baseflow	v_ALPHA_BF.gw	Baseflow alpha factor
	a_GW_DELAY.gw	Groundwater delay
	v_RCHRG_DP.gw	Deep aquifer percolation fraction
	v_REVAPMN.gw	Threshold depth of water in the shallow aquifer for “revap” to occur
	v_GW_REVAP.gw	Groundwater “revap” coefficient
	v_GWQMN.gw	Threshold depth of water in the shallow aquifer required for return flow to occur
Lateral flow	r_LAT_TTIME.hru	Lateral flow travel time
	r_HRU_SLP.hru	Average slope steepness
Channel	r_OV_N.hru	Manning’s coefficient for overland flow
	r_SLSUBBSN.hru	Average slope length
	v_CH_N2.rte	Manning’s coefficient for the main channel
	v_CH_K2.rte	Hydraulic conductivity of the main channel alluvium
Soil	v_ESCO.bsn	Soil evaporation compensation coefficient
	v_EPCO.hru	Plant uptake compensation coefficient
	v_CANMX.hru	Maximum canopy storage
	r_SOL_K.sol	Saturated hydraulic conductivity
	r_SOL_BD.sol	Moist bulk density of the soil layer
	r_SOL_AWC.sol	Soil available water storage capacity

The model performance of each scenario was further analyzed using the coefficient of determination ( $R^2$ ) [45], Nash–Sutcliffe efficiency (NSE) [46], and percent bias (PBIAS) [47], as shown in Equations (2)–(4).

$$R^2 = \frac{[\sum_{i=1}^n (Q_{obs}(i) - \bar{Q}_{obs})(Q_{sim}(i) - \bar{Q}_{sim})]^2}{\sum_{i=1}^n (Q_{obs}(i) - \bar{Q}_{obs})^2 \sum_{i=1}^n (Q_{sim}(i) - \bar{Q}_{sim})^2}, \quad (2)$$

$$NSE = 1 - \left[ \frac{\sum_{i=1}^n (Q_{obs}(i) - Q_{sim}(i))^2}{\sum_{i=1}^n (Q_{obs}(i) - \bar{Q}_{obs})^2} \right], \quad (3)$$

$$\text{PBIAS} = \left[ \frac{\sum_{i=1}^n (Q_{obs}(i) - Q_{sim}(i)) * 100}{\sum_{i=1}^n Q_{obs}(i)} \right], \quad (4)$$

where  $Q_{obs}$  is the measured streamflow,  $Q_{sim}$  is the simulated streamflow on the day  $i$ ,  $\bar{Q}_{obs}$  is the mean of measured streamflow, and  $\bar{Q}_{sim}$  is the mean of simulated streamflow.  $R^2$  varies from 0 to 1, where 0 indicates no correlation and 1 means perfect correlation and less error variance. NSE can vary from  $-\infty$  to 1, where values  $\leq 0$  show that the model is unreliable and values closer to 1 indicate a perfect fit between simulated and measured data. The best PBIAS value is 0. Positive values show that the model results are underestimated, and negative values show that the model results are overestimated. Model performance can be assessed as “satisfactory” for a monthly time step if  $R^2 > 0.60$ ,  $\text{NSE} > 0.50$ , and  $\text{PBIAS} \leq \pm 15\%$  for watershed-scale models [48].

**Table 2.** SWAT calibrated parameters and their sensitivities for each calibration scenario. Numbers in bold indicate the parameters with the highest sensitivity ( $p$ -value  $< 0.03$ ).

Parameters	Initial Ranges		Flow Calibration		AET Calibration		Flow and AET Calibration	
	Min	Max	<i>t</i> -Test	<i>p</i> -Value	<i>t</i> -Test	<i>p</i> -Value	<i>t</i> -Test	<i>p</i> -Value
CN2	−0.10	0.10	−0.85	0.40	1.25	0.21	−0.53	0.59
SURLAG	0.00	10.00	0.38	0.70	0.64	0.53	1.23	0.22
ALPHA_BF	0.00	1.00	−0.07	0.95	0.47	0.64	−0.46	0.65
GW_DELAY	−30.00	90.00	9.89	0.00	−0.82	0.41	9.70	0.00
RCHRG_DP	0.00	0.50	2.78	0.01	−1.24	0.21	2.61	0.01
REVAPMN	800.00	1900.00	0.53	0.60	0.05	0.96	−0.35	0.73
GW_REVAP	0.02	0.20	1.17	0.24	−1.47	0.14	−1.30	0.19
GWQMN	0.00	500.00	0.18	0.86	0.69	0.49	−0.34	0.73
LAT_TTIME	0.00	180.00	18.98	0.00	−0.02	0.99	22.12	0.00
HRU_SLP	−0.50	3.00	6.09	0.00	−7.58	0.00	−8.84	0.00
OV_N	−0.50	3.00	−0.59	0.56	0.37	0.71	0.66	0.51
SLSUBBSN	−0.20	0.20	−2.23	0.03	2.15	0.03	0.17	0.86
CH_N2	0.01	0.30	0.35	0.72	1.56	0.12	1.21	0.23
CH_K2	0.00	127.00	−1.52	0.13	−0.47	0.64	1.60	0.11
ESCO	0.50	0.95	1.70	0.09	29.33	0.00	4.98	0.00
EPCO	0.50	0.95	−0.74	0.46	−5.50	0.00	−0.64	0.52
SOL_K	−0.80	0.80	8.43	0.00	−8.24	0.00	−7.85	0.00
SOL_BD	−0.30	0.30	10.46	0.00	−7.70	0.00	−8.45	0.00
SOL_AWC	−0.05	0.05	−0.34	0.73	0.35	0.72	2.52	0.01

### 3. Results

#### 3.1. Sensitivity Analysis

The most sensitive parameters for each calibration scenario are shown in Table 2. Sensitive parameters are identified by  $p$ -value less than 0.03. Figure A1 shows the relative changes of the five most sensitive parameters for each calibration scenario versus objective function. Most variations of NSE values were found to be in the calibration with streamflow rather than single evapotranspiration and multi-variable calibrations.

In the streamflow calibration, the parameters with the highest sensitivity were lateral flow travel time (LAT\_TTIME), moist bulk density of the soil layer (SOL\_BD), groundwater delay time (GW\_DELAY), saturated hydraulic conductivity (SOL\_K), and average slope steepness (HRU\_SLP). These parameters were connected to groundwater flow, runoff generation, and channel routing. In the AET calibration, the parameters with the highest sensitivity were soil evaporation compensation coefficient (ESCO), saturated hydraulic conductivity (SOL\_K), moist bulk density of the soil layer (SOL\_BD), average slope steepness (HRU\_SLP), and plant uptake compensation coefficient (EPCO), which are mostly related to soil properties. In the multi-variable calibration, the most sensitive parameters were lateral flow travel time (LAT\_TTIME), groundwater delay time (GW\_DELAY), average slope steepness (HRU\_SLP), moist bulk density of the soil layer (SOL\_BD), saturated

hydraulic conductivity (SOL\_K), and soil evaporation compensation coefficient (ESCO). These parameters referred to both groundwater flow and soil properties.

3.2. Model Performance Evaluation

The model performance was assessed with criteria recommended by Moriasi et al. [48]. In all three calibration scenarios, the deviations from the observed values start to increase during the dry season and decline during the wet season. Table 3 displays the model performance for all three scenarios for all the sub-basins. Figure 3 presents the measured and simulated hydrographs at the outlet of the catchment (Monastiri gauging station) for all three scenarios. Finally, Figure 4 shows the measured and simulated AET for the entire study area at a catchment scale.

**Table 3.** Model evaluation statistics for each calibration scenario; (a) Streamflow calibration, (b) AET calibration, and (c) Multi-variable calibration. The location of the sub-basins 1–11 is indicated in Figure 2a–c.

Variable	Station/Sub-Basin	NSE			R <sup>2</sup>			PBIAS (%)		
		(a)	(b)	(c)	(a)	(b)	(c)	(a)	(b)	(c)
Streamflow	Monastiri station	0.71	0.38	0.70	0.84	0.84	0.86	5.60	8.29	6.10
	Sub-basin 1	0.27	0.49	0.18	0.58	0.75	0.57	11.68	11.60	16.70
	Sub-basin 2	0.30	0.33	0.28	0.72	0.76	0.76	10.96	12.70	13.80
	Sub-basin 3	0.11	0.36	−0.10	0.59	0.69	0.55	15.81	15.00	21.70
	Sub-basin 4	0.37	0.34	0.42	0.73	0.75	0.75	8.48	12.50	13.60
	Sub-basin 5	0.09	0.28	0.15	0.80	0.78	0.81	3.07	6.10	5.30
Evapotranspiration	Sub-basin 6	0.22	0.35	0.26	0.64	0.74	0.68	9.00	10.70	14.50
	Sub-basin 7	−0.17	−0.14	0.19	0.87	0.80	0.86	−12.72	−5.30	−8.40
	Sub-basin 8	0.57	0.56	0.69	0.82	0.82	0.83	2.46	6.40	5.40
	Sub-basin 9	0.42	0.51	0.56	0.83	0.82	0.79	2.69	7.00	7.00
	Sub-basin 10	0.44	0.58	0.52	0.80	0.87	0.81	1.19	6.00	4.00
	Sub-basin 11	0.34	0.54	0.63	0.84	0.82	0.83	−0.53	7.70	2.90

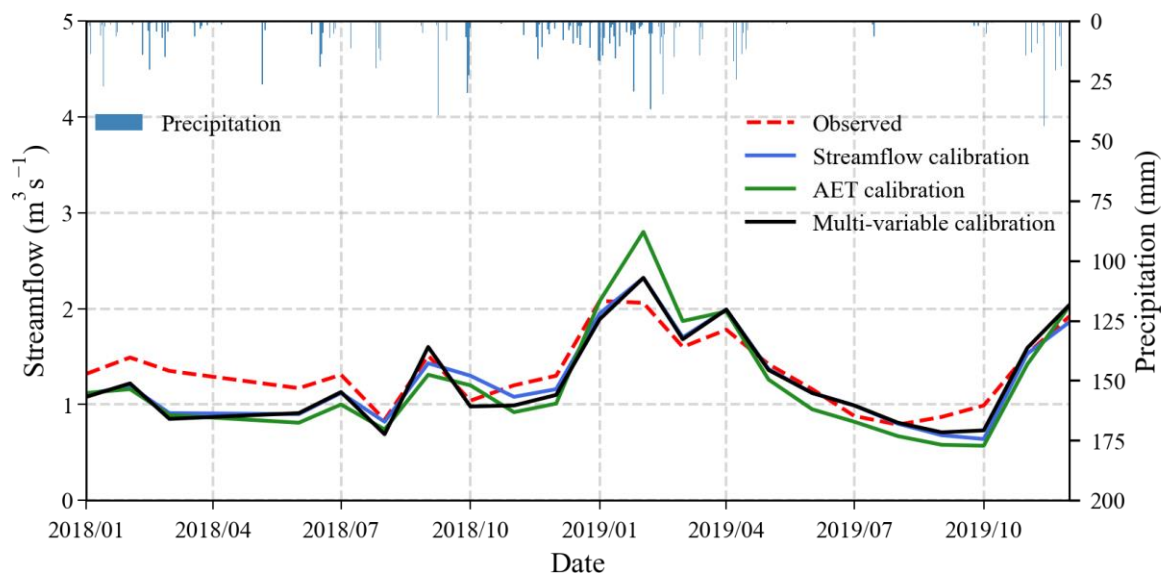


**Figure 3.** Simulated versus measured monthly streamflow for each calibration scenario at the outlet of the sub-basin (Monastiri gauging station).

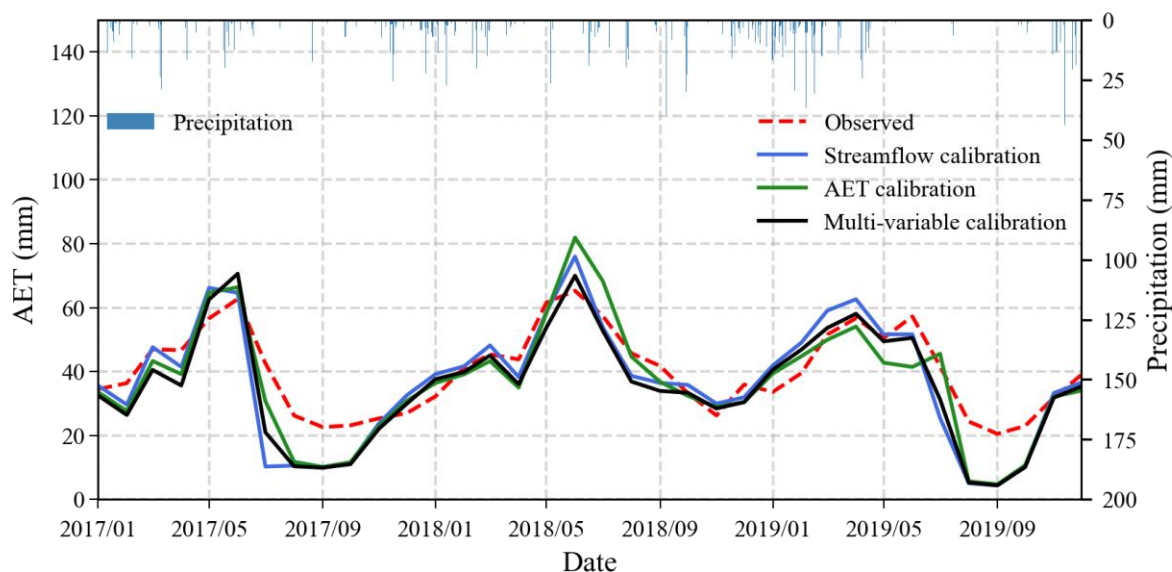


**Figure 4.** Simulated versus measured MODIS evapotranspiration for each calibration scenario at catchment scale.

### 3.2.1. Streamflow Calibration

The streamflow calibration showed good results in general for streamflow ( $NSE = 0.71$ ;  $R^2 = 0.84$ ;  $PBIAS = 5.6\%$ ) (Table 3). The results regarding evapotranspiration were unsatisfactory for  $NSE$  ( $NSE$  within  $-0.17$  to  $0.57$ ), except for sub-basin 8 ( $NSE = 0.57$ ), and satisfactory for  $R^2$  and  $PBIAS$  ( $R^2 > 0.58$ ;  $PBIAS$  within  $-12.7\%$  to  $15.8\%$ ). Figure 3 designates a satisfying match between measured and simulated streamflow except for low flows during the dry season. However, the temporal dynamics of the hydrograph were generated correctly. Figure 4 indicates differences between observed and simulated AET. Streamflow calibration underestimated evapotranspiration in the wet season and overestimated evapotranspiration at the beginning of the dry season.

### 3.2.2. Actual Evapotranspiration Calibration

The AET calibration presented unsatisfactory performance for  $NSE$  for sub-basins 2–7 and satisfactory performance for sub-basins 1, 8, 9, 10, and 11 ( $NSE$  within  $-0.14$  to  $0.58$ ) (Table 3). In respect of  $R^2$  and  $PBIAS$ , the results were satisfactory for all the sub-basins ( $R^2 > 0.69$ ;  $PBIAS$  within  $-5.3\%$  to  $15\%$ ). The performance for streamflow was unsatisfactory ( $NSE = 0.38$ ;  $R^2 = 0.84$ ;  $PBIAS = 8.3\%$ ). In particular, the observed and simulated AET values did not match well. Nevertheless, they showed a well-matched seasonal variation of evapotranspiration (Figure 4). AET calibration underestimated low flows and overestimated high flows for the simulation period (Figure 3). Performance statistics were generally better for streamflow than evapotranspiration in single-variable calibration scenarios.

### 3.2.3. Multi-Variable Calibration

The multi-variable scenario, using streamflow and MODIS satellite-based AET, showed satisfactory performance for streamflow ( $NSE = 0.70$ ;  $R^2 = 0.86$ ;  $PBIAS = 6.1\%$ ) and unsatisfactory (sub-basins 1–7) to satisfactory (sub-basins 8–11) performance for evapotranspiration ( $NSE$  within  $-0.10$  to  $0.69$ ;  $R^2 > 0.55$ ;  $PBIAS$  within  $-8.4\%$  to  $21.7\%$ ) (Table 3). Simulated and observed streamflow values are much better than those for AET calibration and similar to streamflow calibration (Figure 3). Results for AET are related to those of AET calibration, showing underestimation of the simulated values (Figure 4). Compared to single variable calibration scenarios, multi-variable calibration displayed similar  $NSE$  values obtained from single-variable calibration, and  $R^2$  showed good performances ( $>0.75$ ) for both variables (Table 3).

### 3.3. Major Water Balance Components

The major water balance components (i.e., actual evapotranspiration, water yield, and precipitation) are displayed in Figure 5. In general, average annual precipitation (643 mm) was slightly greater than combined water yield (WYLD) and actual evapotranspiration (AET) values. Actual evapotranspiration contributed a large amount of water loss from the watershed, about 60% in all scenarios. The total water yield of the multi-variable calibration is higher than the other two modeling scenarios. In particular, the total water yield was estimated to be 171 mm for flow calibration, 151 mm for AET calibration, and 186 mm for multi-variable calibration.

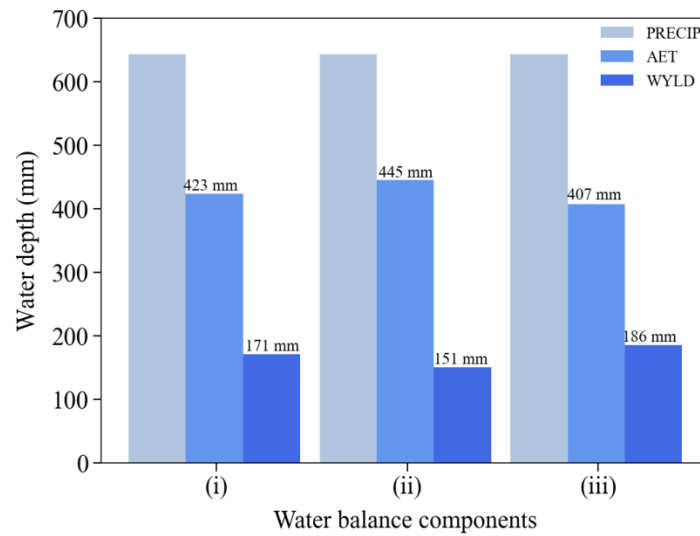


**Figure 5.** Water balance components; (i) Streamflow calibration, (ii) AET calibration, and (iii) Multi-variable calibration. PRECIP: Precipitation (mm), AET: Actual evapotranspiration (mm), WYLD: Water yield (mm).

## 4. Discussion

In this study, the SWAT hydrological model was used to interpret the behaviour of an urban/sub-urban environment and analyse its underlying mechanisms. The study area is a typical Mediterranean catchment prone to natural hazards such as floods, forest fires and their combined impact. Therefore, the mechanisms governing surface runoff and the interactions between the hydrological components should be analysed in depth for these vulnerable areas. The main objective was to investigate which parameters are more sensitive in a mixed land-use basin and to propose a multi-variable calibration procedure using both streamflow and satellite-based AET data for SWAT modelling.

The sensitivity analysis results showed that the parameters with the highest sensitivity for streamflow are connected to groundwater flow, runoff generation, and channel routing, and for actual evapotranspiration, they are linked to soil properties, respectively (Table 2, Figure A1). The differences in the sensitivity of the parameters are due to different data used in the calibration process. Similar outcomes were obtained by Sirisena et al. [16] and Moriasi et al. [49]. Sirisena et al. [16] concluded that the most sensitive parameters for evapotranspiration were connected to soil properties. Moriasi et al. [49] pointed out that the high sensitivity of the soil parameters to AET indicated a connection between actual evaporation and soil water.

Both variables present a slightly better performance in the single calibrations with streamflow and evapotranspiration than in the multi-variable calibration (Table 3). Nonetheless, the multi-variable calibration produced satisfactory results for both streamflow and AET and showed reasonably good streamflow estimations (NSE = 0.70). AET showed the best performance for forests (e.g., sub-basins 1, 8, 9, 10, 11). This indicates that the MODIS data probably show better performance at simulating forests and semi-natural

areas than in sub-urban areas, including more complex management systems. In addition, evapotranspiration algorithms are characterized by resolution issues, misclassification of land use, and data generation uncertainties [50]. Therefore, these algorithms may not correctly capture the land use changes (especially in sub-urban areas) and the available soil moisture on the ground.

In most sub-basins, MODIS satellite-based AET and SWAT simulated AET show that seasonal patterns match well, although the SWAT model under-predicted AET compared with the MODIS satellite-based AET during the dry season (Figure 4, Table 3). These results are consistent with those of other studies [51,52]. A study in Morocco [51] and a study in Iran [52] suggested that the multi-variable calibration can produce good results for both variables. Nevertheless, the single variable calibrations showed better performance. The differences for all three scenarios intensify during the dry season and decline during the wet season (Figures 3 and 4). The underestimation of AET and the low baseflow, especially during the dry season (Figure 3), could suggest unknown water contributions in the study area. These deviations are probably also connected to soil replenishment and the crops' high water demand during the dry season. Furthermore, it is worth mentioning that MODIS satellite-based AET could include errors and underestimations or overestimations of the "true" AET, altering the model's water balance [53]. For instance, the higher MODIS satellite-based AET values in the AET calibration scenario led to lower water yield values than the streamflow calibration scenario (Figure 5). Satellite-based evapotranspiration datasets use sensor-derived parameters (e.g., surface heat flux, latent heat flux) that may have several uncertainties. Model misrepresentations, errors in the inputs, and spatial and temporal scaling decrease the efficiency of the algorithms [54].

For both single variable calibrations, the simulated second variable (i.e., AET for streamflow calibration and streamflow for AET calibration) is not well represented. The unsatisfactory performance of the second variable in the single variable calibrations indicates the poor representation of the catchment's water balance. Many studies support that incorporating satellite data in the hydrological model calibration improved the estimation of water balance components regardless of the model performance improvement. A study in China [55] calibrated the SWAT model with GLEAM AET data and streamflow. Although streamflow only calibration produced reliable results, this approach grouped the hydrological process. Furthermore, a study by Immerzeel and Droogers [13] pointed out that incorporating AET data in hydrological model calibration reduces equifinality obtained from traditional streamflow only calibration. The water balance is best reproduced when both streamflow and AET are used in the calibration process [52]. Several studies [49,56] reported that satellite AET data could be used to constrain hydrological parameters that are highly sensitive to evapotranspiration.

In general, the calibration process is challenging because of the uncertainties that exist due to model simplification, processes that are not accounted by the model, and processes that are unknown to the modeler [14]. In this study, the main sources of uncertainty are connected to inaccuracies (i) in the quality of input data (climate, soil, and land cover resolution), (ii) in the model set up (aggregation and interpolation methods), (iii) in the choice of objective data and parameterization, (iv) observed data, and (v) processes unknown to the modeler which interfere with the natural system [42]. Observational errors in the precipitation data, MODIS actual evapotranspiration, and discharge, as well as the effects of elevation and topography, increase bias and generate variability. For example, errors in streamflow measurements can vary from 6% to 19% under different combinations of channel types and measurement techniques [57]. In addition, poor resolution and data generation uncertainties in evapotranspiration algorithms can induce biases between AET simulated values and satellite-based AET [17,50,58]. For instance, a study in Ethiopia [50] estimated the major water balance components of the Upper Blue Nile basin using the JGrass-NewAge hydrological system and remote sensing data (GLEAM and MODIS AET). This study concluded that the satellite-based data introduce bias in estimating the water budget. Another study by [58] conducted a multi-objective validation for West Africa river

basins using remote sensing data. The results showed that MODIS satellite-based AET underestimated SWAT-simulated AET in arid areas. Finally, Dile et al. [17] evaluated AET outputs derived from AVHRR and MOD16 AET datasets using outputs from a SWAT model for Ethiopia. This study suggested that datasets did not agree well with the precipitation in regions with a bimodal precipitation pattern. Therefore, careful consideration should be given to analyzing data from satellite-based products. Further information is necessary to estimate the uncertainty in model outputs and improve the calibration results at HRU level.

## 5. Conclusions

This study used monthly streamflow and MODIS satellite-based AET data to calibrate the SWAT model. Three calibration scenarios were conducted with streamflow, AET, and streamflow–AET data to evaluate the simulated outputs. The sensitivity analysis showed that the most sensitive parameters for streamflow are related to groundwater flow, runoff generation, and channel routing, and for actual evapotranspiration, they are all connected to soil properties. The model performance results indicated that the single variable calibrations showed satisfactory performance only for the first variable that was simulated. The multi-variable calibration showed satisfactory performance for both streamflow and AET. The SWAT model generally under-predicted AET in all scenarios compared to MODIS satellite-based AET.

This research showed that combining streamflow and MODIS satellite-based AET data in the calibration process can improve model performance regarding streamflow and water balance and contribute to understanding the hydrological processes in a mixed land-use catchment. Furthermore, the use of satellite data in model calibration, as presented in this study, can be utilized in catchments lacking measured data or in catchments with similar hydrological and geomorphological characteristics. Future work should incorporate discharge, soil moisture, and HRU level AET data in a combined objective function at a high temporal resolution.

**Author Contributions:** Conceptualization, E.K. and A.K.; methodology, E.K. and A.K.; software, E.K.; validation, E.K.; formal analysis, E.K.; investigation, E.K.; resources, E.K. and A.K.; data curation, E.K.; writing—original draft preparation, E.K.; writing—review and editing, E.K. and A.K.; visualization, E.K.; supervision, A.K.; project administration, A.K.; funding acquisition, A.K. All authors have read and agreed to the published version of the manuscript.

**Funding:** The research work was supported by the Hellenic Foundation for Research and Innovation (HFRI) under the HFRI PhD Fellowship grant (Fellowship Number: 1586).

**Institutional Review Board Statement:** Not applicable.

**Informed Consent Statement:** Not applicable.

**Data Availability Statement:** The SWAT model is available at the website <http://swat.tamu.edu/> (accessed on 10 December 2020) (USDA Agricultural Research Service). The DEM data were obtained from the website <https://earthexplorer.usgs.gov/> (accessed on 22 December 2020) (Shuttle Radar Topography Mission, SRTM). The land use data were downloaded from the website <https://land.copernicus.eu/> (accessed on 22 December 2020) (Corine Land Cover, CLC 2018). The soil data were downloaded from the website <http://www.fao.org/> (accessed on 22 December 2020) (Food and Agriculture Organization, FAO). The meteorological data were downloaded from the website <https://www.meteo.gr/> (accessed on 11 January 2021) (National Observatory of Athens, NOA). The streamflow data were obtained from the website <https://openhi.net/> (accessed on 20 January 2021) (Open Hydrosystem Information Network). The AET data were downloaded from the website <https://modis.gsfc.nasa.gov/> (accessed on 14 March 2021) (Moderate Resolution Imaging Spectroradiometer).

**Acknowledgments:** The authors are grateful to Nancy Sammons, Information Technology Specialist of the SWAT team for her kind help with the SWAT software. Authors gratefully acknowledge the financial support from the Hellenic Foundation for Research and Innovation (HFRI).

**Conflicts of Interest:** The authors declare no conflict of interest. The funders had no role in the design of the study; in the collection, analyses, or interpretation of data; in the writing of the manuscript, or in the decision to publish the results.

## Appendix A

The following tables display the land use categories of the study area at catchment (Table A1) and sub-basin level (Table A2).

**Table A1.** Land use categories of the study area at catchment level.

Corine Classification	SWAT Code	SWAT Classification	(%) Catchment
Industrial or commercial units	UCOM	Commercial	11.43
Discontinuous urban fabric	URLD	Residential-Low Density	34.11
Road and rail networks and associated land	UTRN	Transportation	4.07
Continuous urban fabric	URHD	Residential-High Density	1.54
Pastures	PAST	Pasture	0.31
Land principally occupied by agriculture, with significant areas of natural vegetation	AGRL	Agricultural Land-Generic	12.39
Broad-leaved forest	FRSD	Forest-Deciduous	3.11
Coniferous forest	FRSE	Forest-Evergreen	9.59
Mixed forest	FRST	Forest-Mixed	7.51
Sclerophyllous vegetation	RNGB	Range-Brush	15.94

**Table A2.** Land use categories of the study area at sub-basin level. Artificial surfaces (i.e., urban fabric, industrial, commercial and transport units), agricultural areas (i.e., arable land, pastures and heterogeneous agricultural areas) and forests and semi natural areas (i.e., forests, scrub and herbaceous vegetation associations).

Sub-Basins	Artificial Surfaces (%)	Agricultural Areas (%)	Forests and Semi Natural Areas (%)
Sub-basin 1	1.88	5.02	93.10
Sub-basin 2	53.36	9.95	36.69
Sub-basin 3	21.83	9.28	68.89
Sub-basin 4	56.11	25.05	18.84
Sub-basin 5	76.91	0.74	22.35
Sub-basin 6	18.31	23.25	58.45
Sub-basin 7	76.43	8.34	15.23
Sub-basin 8	56.77	0.29	42.94
Sub-basin 9	75.28	3.06	21.65
Sub-basin 10	80.65	2.72	16.63
Sub-basin 11	28.65	27.38	43.97
Sub-basin 12	100.01	0.00	0.00
Sub-basin 13	74.16	25.83	0.00
Sub-basin 14	73.29	26.71	0.00
Sub-basin 15	81.90	18.10	0.00
Sub-basin 16	99.33	0.67	0.00
Sub-basin 17	64.20	35.76	0.04
Sub-basin 18	29.88	19.13	51.00
Sub-basin 19	7.98	13.54	78.48
Sub-basin 20	9.29	28.47	62.23
Sub-basin 21	80.42	19.58	0.00
Sub-basin 22	73.64	26.36	0.00
Sub-basin 23	83.87	16.13	0.00
Sub-basin 24	100.01	0.00	0.00
Sub-basin 25	100.00	0.00	0.00

The following figure shows the relative changes of the five most sensitive parameters for each calibration scenario versus objective function (Figure A1).

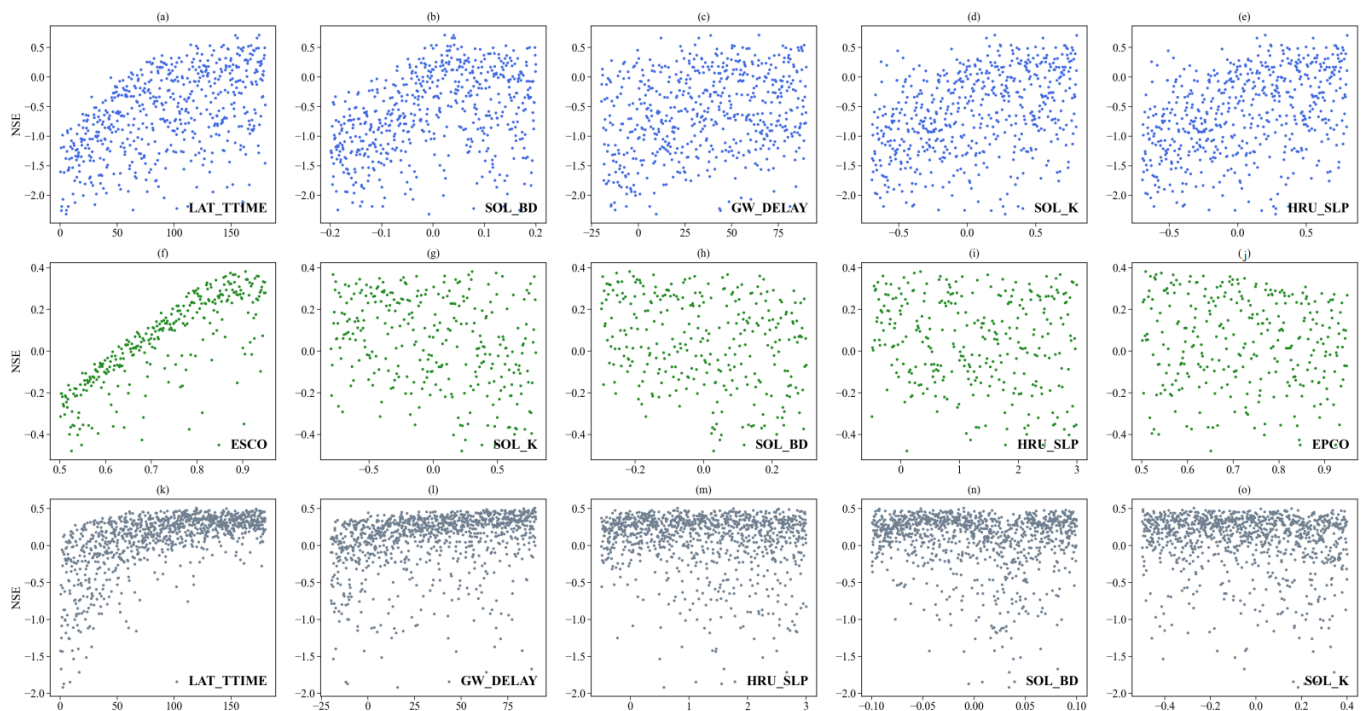


**Figure A1.** Calibrated values ( $x$ -axis) versus objective function NSE value range ( $y$ -axis); blue dots symbolize streamflow calibration, green dots symbolize AET calibration, and grey dots symbolize multi-variable calibration. The parameters (a–e) are the most sensitive parameters for streamflow calibration, the parameters (f–j) are the most sensitive parameters for AET calibration, and the parameters (k–o) are the most sensitive parameters for multi-variable calibration.

## References

1. Arnold, J.G.; Youssef, M.A.; Yen, H.; White, M.J.; Sheshukov, A.Y.; Sadeghi, A.M.; Moriasi, D.N.; Steiner, J.L.; Amatya, D.M.; Skaggs, R.W.; et al. Hydrological Processes and Model Representation: Impact of Soft Data on Calibration. *Trans. ASABE* **2015**, *58*, 1637–1660. [[CrossRef](#)]
2. Daggupati, P.; Yen, H.; White, M.J.; Srinivasan, R.; Arnold, J.G.; Keitzer, C.S.; Sowa, S.P. Impact of model development, calibration and validation decisions on hydrological simulations in West Lake Erie Basin. *Hydrol. Processes* **2015**, *29*, 5307–5320. [[CrossRef](#)]
3. Gassman, P.W.; Sadeghi, A.M.; Srinivasan, R. Applications of the SWAT Model Special Section: Overview and Insights. *J. Environ. Qual.* **2014**, *43*, 1–8. [[CrossRef](#)] [[PubMed](#)]
4. Hrachowitz, M.; Savenije, H.H.G.; Blöschl, G.; McDonnell, J.J.; Sivapalan, M.; Pomeroy, J.W.; Arheimer, B.; Blume, T.; Clark, M.P.; Ehret, U.; et al. A decade of Predictions in Ungauged Basins (PUB)—A review. *Hydrol. Sci. J.* **2013**, *58*, 1198–1255. [[CrossRef](#)]
5. Van Emmerik, T.; Mulder, G.; Eilander, D.; Piet, M.; Savenije, H. Predicting the ungauged basin: Model validation and realism assessment. *Front. Earth Sci.* **2015**, *3*, 62. [[CrossRef](#)]
6. Arnold, J.G.; Moriasi, D.N.; Gassman, P.W.; Abbaspour, K.C.; White, M.J.; Srinivasan, R.; Santhi, C.; Harmel, R.D.; Van Griensven, A.; Van Liew, M.W.; et al. SWAT: Model Use, Calibration, and Validation. *Trans. ASABE* **2012**, *55*, 1491–1508. [[CrossRef](#)]
7. Beven, K.; Binley, A. GLUE: 20 years on. *Hydrol. Processes* **2014**, *28*, 5897–5918. [[CrossRef](#)]
8. Kelleher, C.; McGlynn, B.; Wagener, T. Characterizing and reducing equifinality by constraining a distributed catchment model with regional signatures, local observations, and process understanding. *Hydrol. Earth Syst. Sci.* **2017**, *21*, 3325–3352. [[CrossRef](#)]
9. Liu, Z.; Yin, J.; Dahlke, H.E. Enhancing Soil and Water Assessment Tool Snow Prediction Reliability with Remote-Sensing-Based Snow Water Equivalent Reconstruction Product for Upland Watersheds in a Multi-Objective Calibration Process. *Water* **2020**, *12*, 3190. [[CrossRef](#)]
10. Her, Y.; Seong, C. Responses of hydrological model equifinality, uncertainty, and performance to multi-objective parameter calibration. *J. Hydroinformatics* **2018**, *20*, 864–885. [[CrossRef](#)]
11. Rajib, A.; Merwade, V.; Yu, Z. Rationale and Efficacy of Assimilating Remotely Sensed Potential Evapotranspiration for Reduced Uncertainty of Hydrologic Models. *Water Resour. Res.* **2018**, *54*, 4615–4637. [[CrossRef](#)]
12. Shah, S.; Duan, Z.; Song, X.; Li, R.; Mao, H.; Liu, J.; Ma, T.; Wang, M. Evaluating the added value of multi-variable calibration of SWAT with remotely sensed evapotranspiration data for improving hydrological modeling. *J. Hydrol.* **2021**, *603*, 127046. [[CrossRef](#)]
13. Immerzeel, W.W.; Droogers, P. Calibration of a distributed hydrological model based on satellite evapotranspiration. *J. Hydrol.* **2008**, *349*, 411–424. [[CrossRef](#)]

14. Abbaspour, K.C.; Yang, J.; Maximov, I.; Siber, R.; Bogner, K.; Mieleitner, J.; Zobrist, J.; Srinivasan, R. Modelling hydrology and water quality in the pre-alpine/alpine Thur watershed using SWAT. *J. Hydrol.* **2007**, *333*, 413–430. [CrossRef]
15. Parajuli, P.B.; Jayakody, P.; Ouyang, Y. Evaluation of Using Remote Sensing Evapotranspiration Data in SWAT. *Water Resour. Manag.* **2018**, *32*, 985–996. [CrossRef]
16. Sirisena, T.A.J.G.; Maskey, S.; Ranasinghe, R. Hydrological Model Calibration with Streamflow and Remote Sensing Based Evapotranspiration Data in a Data Poor Basin. *Remote Sens.* **2020**, *12*, 3768. [CrossRef]
17. Dile, Y.T.; Ayana, E.K.; Worqlul, A.W.; Xie, H.; Srinivasan, R.; Lefore, N.; You, L.; Clarke, N. Evaluating satellite-based evapotranspiration estimates for hydrological applications in data-scarce regions: A case in Ethiopia. *Sci. Total Environ.* **2020**, *743*, 140702. [CrossRef]
18. Herman, M.R.; Nejadhashemi, A.P.; Abouali, M.; Hernandez-Suarez, J.S.; Daneshvar, F.; Zhang, Z.; Anderson, M.C.; Sadeghi, A.M.; Hain, C.R.; Sharifi, A. Evaluating the role of evapotranspiration remote sensing data in improving hydrological modeling predictability. *J. Hydrol.* **2018**, *556*, 39–49. [CrossRef]
19. Aboelnour, M.; Gitau, M.W.; Engel, B.A. Hydrologic response in an urban watershed as affected by climate and land-use change. *Water* **2019**, *11*, 1603. [CrossRef]
20. Becker, R.; Koppa, A.; Schulz, S.; Usman, M.; aus der Beek, T.; Schüth, C. Spatially distributed model calibration of a highly managed hydrological system using remote sensing-derived ET data. *J. Hydrol.* **2019**, *577*, 123944. [CrossRef]
21. Busico, G.; Colombani, N.; Fronzi, D.; Pellegrini, M.; Tazioli, A.; Mastrocicco, M. Evaluating SWAT model performance, considering different soils data input, to quantify actual and future runoff susceptibility in a highly urbanized basin. *J. Environ. Manag.* **2020**, *266*, 110625. [CrossRef] [PubMed]
22. Jha, M.K.; Afreen, S. Flooding urban landscapes: Analysis using combined hydrodynamic and hydrologic modeling approaches. *Water* **2020**, *12*, 1986. [CrossRef]
23. van Tol, J.; van Zijl, G.; Julich, S. Importance of detailed soil information for hydrological modelling in an urbanized environment. *Hydrology* **2020**, *7*, 34. [CrossRef]
24. Boithias, L.; Sauvage, S.; Lenica, A.; Roux, H.; Abbaspour, K.; Larnier, K.; Dartus, D.; Sánchez-Pérez, J. Simulating Flash Floods at Hourly Time-Step Using the SWAT Model. *Water* **2017**, *9*, 929. [CrossRef]
25. Mamassis, N.; Koukouvinos, A.; Baki, S. *Final Report, Development of a Geographical Information System and an Internet Application for the Supervision of Kephisos Protected Areas*; Department of Water Resources and Environmental Engineering, National Technical University of Athens: Athens, Greece, 2008; Available online: [http://www.itia.ntua.gr/el/project\\_reports/151/](http://www.itia.ntua.gr/el/project_reports/151/) (accessed on 15 January 2021).
26. Zerefos, C.; Repapis, C.; Giannakopoulos, C.; Kapsomenakis, J.; Papanikolaou, D.; Papanikolaou, M.; Poulos, S.; Vrekoussis, M.; Philandras, C.; Tselioudis, G. The climate of the Eastern Mediterranean and Greece: Past, present and future. In *The Environmental, Economic and Social Impacts of Climate Change in Greece*; Bank of Greece: Athens, Greece, 2011; pp. 50–58.
27. Lagouvardos, K.; Kotroni, V.; Bezes, A.; Koletsis, I.; Kopania, T.; Lykoudis, S.; Mazarakis, N.; Papagiannaki, K.; Vougioukas, S. The automatic weather stations NOANN network of the National Observatory of Athens: Operation and database. *Geosci. Data J.* **2017**, *4*, 4–16. [CrossRef]
28. Corine Land Cover, (CLC) Land Use Data. Available online: <https://land.copernicus.eu/> (accessed on 15 December 2020).
29. Food and Agriculture Organization, (FAO). HWSO Soil Data. Available online: [www.fao.org](http://www.fao.org) (accessed on 10 December 2020).
30. U.S. Geological Survey, (USGS). Shuttle Radar Topography Mission (SRTM), DEM Data. Available online: <https://earthexplorer.usgs.gov/> (accessed on 5 December 2020).
31. FAO; IIASA; ISRIC; ISSCAS. *Harmonized World Soil Database Version 1.2*; Food & Agriculture Organization of the UN: Rome, Italy; International Institute for Applied Systems Analysis: Laxenburg, Austria, 2012; ISBN 9781626239777.
32. Open Hydrosystem Information Network, (OpenHi.net). Observed Streamflow Data. Available online: <https://openhi.net/> (accessed on 20 December 2020).
33. Moderate Resolution Imaging Spectroradiometer, (MODIS). Evapotranspiration Data. Available online: <https://modis.gsfc.nasa.gov/> (accessed on 2 March 2021).
34. Running, S.; Mu, Q.; Zhao, M.; Moreno, A. *User's Guide NASA Earth Observing System MODIS Land Algorithm (For Collection 6)*; National Aeronautics and Space Administration (NASA): Washington, DC, USA, 2019; pp. 1–38.
35. Arnold, J.G.; Srinivasan, R.; Muttiah, R.S.; Williams, J.R. Large Area Hydrologic Modeling and Assessment Part I: Model Development. *J. Am. Water Resour. Assoc.* **1998**, *34*, 73–89. [CrossRef]
36. Neitsch, S.L.; Arnold, J.G.; Kiniry, J.R.; Williams, J.R. *Soil & Water Assessment Tool Theoretical Documentation Version 2009*; Texas Water Resources Institute: Texas, TX, USA, 2011; ISBN Technical Report No. 406.
37. Gassman, P.W.; Reyes, M.R.; Green, C.H.; Arnold, J.G. The Soil and Water Assessment Tool: Historical Development, Applications, and Future Research Directions. *Trans. ASABE* **2007**, *50*, 1211–1250. [CrossRef]
38. Dile, Y.T.; Daggupati, P.; George, C.; Srinivasan, R.; Arnold, J. Introducing a new open source GIS user interface for the SWAT model. *Environ. Model. Softw.* **2016**, *85*, 129–138. [CrossRef]
39. Soil Conservation Service, S. *National Engineering Handbook, Section 4, Hydrology*; Department of Agriculture: Washington, DC, USA, 1972.
40. Jeong, J.; Williams, J.R.; Merkel, W.H.; Arnold, J.G.; Wang, X.; Rossi, C.G. Improvement of the variable storage coefficient method with water surface gradient as a variable. *Trans. ASABE* **2014**, *57*, 791–801. [CrossRef]
41. Abbaspour, K.C.; Johnson, C.A.; van Genuchten, M.T. Estimating Uncertain Flow and Transport Parameters Using a Sequential Uncertainty Fitting Procedure. *Vadose Zone J.* **2004**, *3*, 1340–1352. [CrossRef]

42. Abbaspour, K.C.; Rouholahnejad, E.; Vaghefi, S.; Srinivasan, R.; Yang, H.; Kløve, B. A continental-scale hydrology and water quality model for Europe: Calibration and uncertainty of a high-resolution large-scale SWAT model. *J. Hydrol.* **2015**, *524*, 733–752. [[CrossRef](#)]
43. Odusanya, A.E.; Mehdi, B.; Schürz, C.; Oke, A.O.; Awokola, O.S.; Awomeso, J.A.; Adejuwon, J.O.; Schulz, K. Multi-site calibration and validation of SWAT with satellite-based evapotranspiration in a data-sparse catchment in southwestern Nigeria. *Hydrol. Earth Syst. Sci.* **2019**, *23*, 1113–1144. [[CrossRef](#)]
44. Franco, A.C.L.; Bonumá, N.B. Multi-variable SWAT model calibration with remotely sensed evapotranspiration and observed flow. *RBRH* **2017**, *22*, 1–14. [[CrossRef](#)]
45. Moriasi, D.N.; Arnold, J.G.; Van Liew, M.W.; Bingner, R.L.; Harmel, R.D.; Veith, T.L. Model Evaluation Guidelines for Systematic Quantification of Accuracy in Watershed Simulations. *Trans. ASABE* **2007**, *50*, 885–900. [[CrossRef](#)]
46. Nash, J.E.; Sutcliffe, J.V. River flow forecasting through conceptual models part I—A discussion of principles. *J. Hydrol.* **1970**, *10*, 282–290. [[CrossRef](#)]
47. Gupta, H.V.; Sorooshian, S.; Yapo, P.O. Status of Automatic Calibration for Hydrologic Models: Comparison with Multilevel Expert Calibration. *J. Hydrol. Eng.* **1999**, *4*, 135–143. [[CrossRef](#)]
48. Moriasi, D.N.; Gitau, M.W.; Pai, N.; Daggupati, P. Hydrologic and water quality models: Performance measures and evaluation criteria. *Trans. ASABE* **2015**, *58*, 1763–1785. [[CrossRef](#)]
49. Tobin, K.; Bennett, M. Improving Alpine Summertime Streamflow Simulations by the Incorporation of Evapotranspiration Data. *Water* **2019**, *11*, 112. [[CrossRef](#)]
50. Abera, W.; Formetta, G.; Brocca, L.; Rigon, R. Modeling the water budget of the Upper Blue Nile basin using the JGrass-NewAge model system and satellite data. *Hydrol. Earth Syst. Sci.* **2017**, *21*, 3145–3165. [[CrossRef](#)]
51. López López, P.; Sutanudjaja, E.H.; Schellekens, J.; Sterk, G.; Bierkens, M.F.P. Calibration of a large-scale hydrological model using satellite-based soil moisture and evapotranspiration products. *Hydrol. Earth Syst. Sci.* **2017**, *21*, 3125–3144. [[CrossRef](#)]
52. Rientjes, T.H.M.; Muthuwatta, L.P.; Bos, M.G.; Booij, M.J.; Bhatti, H.A. Multi-variable calibration of a semi-distributed hydrological model using streamflow data and satellite-based evapotranspiration. *J. Hydrol.* **2013**, *505*, 276–290. [[CrossRef](#)]
53. Vervoort, W.R.; Miechels, S.F.; van Ogtrop, F.F.; Guillaume, J.H.A. Remotely sensed evapotranspiration to calibrate a lumped conceptual model: Pitfalls and opportunities. *J. Hydrol.* **2014**, *519*, 3223–3236. [[CrossRef](#)]
54. Ferguson, C.R.; Sheffield, J.; Wood, E.F.; Gao, H. Quantifying uncertainty in a remote sensing-based estimate of evapotranspiration over continental USA. *Int. J. Remote Sens.* **2010**, *31*, 3821–3865. [[CrossRef](#)]
55. Jin, X.; Jin, Y. Calibration of a Distributed Hydrological Model in a Data-Scarce Basin Based on GLEAM Datasets. *Water* **2020**, *12*, 897. [[CrossRef](#)]
56. Tobin, K.J.; Bennett, M.E. Constraining SWAT Calibration with Remotely Sensed Evapotranspiration Data. *J. Am. Water Resour. Assoc.* **2017**, *53*, 593–604. [[CrossRef](#)]
57. Harmel, R.D.; Cooper, R.J.; Slade, R.M.; Haney, R.L.; Arnold, J.G. Cumulative uncertainty in measured streamflow and water quality data for small watersheds. *Trans. ASABE* **2006**, *49*, 689–701. [[CrossRef](#)]
58. Poméon, T.; Diekkrüger, B.; Springer, A.; Kusche, J.; Eicker, A. Multi-Objective Validation of SWAT for Sparsely-Gauged West African River Basins—A Remote Sensing Approach. *Water* **2018**, *10*, 451. [[CrossRef](#)]